

Interrogation of optical Ramsey spectrum and stability study of an ^{87}Sr optical lattice clock

Jing-Jing Xia(夏京京), Xiao-Tong Lu(卢晓同), and Hong Chang(常宏)
Citation: Chin. Phys. B, 2022, 31 (**3**): 034209. DOI: 10.1088/1674-1056/ac11e0
Journal homepage: http://cpb.iphy.ac.cn; http://iopscience.iop.org/cpb

What follows is a list of articles you may be interested in

Improved thermal property of strained InGaAlAs/AlGaAs quantum wells for 808-nm vertical cavity surface emitting lasers

Zhuang-Zhuang Zhao(赵壮壮), Meng Xun(荀孟), Guan-Zhong Pan(潘冠中), Yun Sun(孙昀), Jing-Tao Zhou(周静涛), and De-Xin Wu(吴德馨)
Chin. Phys. B, 2022, 31 (**3**): 034208. DOI: 10.1088/1674-1056/ac16d0

High sensitivity plasmonic temperature sensor based on a side-polished photonic crystal fiber

Zhigang Gao(高治刚), Xili Jing(井西利), Yundong Liu(刘云东), Hailiang Chen(陈海良), and Shuguang Li(李曙光)
Chin. Phys. B, 2022, 31 (**2**): 024207. DOI: 10.1088/1674-1056/ac0a63

Tunable optomechanically induced transparency and fast-slow light in a loop-coupled optomechanical system

Qinghong Liao(廖庆洪), Xiaoqian Wang(王晓倩), Gaoqian He(何高倩), and Liangtao Zhou(周良涛)
Chin. Phys. B, 2021, 30 (**9**): 094205. DOI: 10.1088/1674-1056/ac0cda

A low-threshold multiwavelength Brillouin fiber laser with double-frequency spacing based on a small-core fiber

Lu-Lu Xu(徐路路), Ying-Ying Wang(王莹莹), Li Jiang(江丽), Pei-Long Yang(杨佩龙), Lei Zhang(张磊), and Shi-Xun Dai(戴世勋)
Chin. Phys. B, 2021, 30 (**8**): 084210. DOI: 10.1088/1674-1056/abff47

Modeling of cascaded high isolation bidirectional amplification in long-distance fiber-optic time and frequency synchronization system

Kuan-Lin Mu(穆宽林), Xing Chen(陈星), Zheng-Kang Wang(王正康), Yao-Jun Qiao(乔耀军), and Song Yu(喻松)
Chin. Phys. B, 2021, 30 (**7**): 074208. DOI: 10.1088/1674-1056/abf105

Interrogation of optical Ramsey spectrum and stability study of an ^{87}Sr optical lattice clock

Jing-Jing Xia(夏京京)[1], Xiao-Tong Lu(卢晓同)[1,2], and Hong Chang(常宏)[1,2,†]

[1] *CAS Key Laboratory of Time and Frequency Primary Standards, National Time Service Center, Xi'an* 710600, *China*
[2] *University of Chinese Academy of Sciences (CAS), Beijing* 100049, *China*

(Received 31 May 2021; revised manuscript received 1 July 2021; accepted manuscript online 7 July 2021)

The optical Ramsey spectrum is experimentally realized in an ^{87}Sr optical lattice clock, and the measured linewidth agrees well with theoretical expectation. The coherence time between the clock laser and the atoms, which indicates the maximum free evolution period of using Ramsey detection to measure the atom-laser phase information, is determined as 340(23) ms by measuring the fringe contrasts of the Ramsey spectrum as a function of the free evolution period. Furthermore, with the same clock duty cycle of about 0.1, the clock stability is measured by using the Ramsey and Rabi spectra, respectively. The experimental and theoretical results show approximately the same stability as the two detection methods, which indicates that Ramsey detection cannot obviously improve the clock stability until the clock duty cycle is large enough. Thus, it is of great significance to choose the detection method of a specific clock.

Keywords: optical Ramsey spectrum, optical lattice clock, stability, coherence time

PACS: 42.62.Fi, 95.55.Sh, 42.62.Eh, 42.50.Gy **DOI:** 10.1088/1674-1056/ac11e0

1. Introduction

Atomic clocks have developed rapidly due to advances in atoms, and optical and quantum science,[1,2] while research on atomic clocks has also promoted the development of scientific frontiers, affecting both basic and applied research. Nowadays, the time frequency standard plays a key role in many important fields, such as satellite navigation,[3] deep space exploration,[4] geodesy[5] and the verification of basic physical theory.[6,7] Thus, the optical clock based on optical frequency transition, which is at least four orders of magnitude higher than that of a microwave clock, has become the focus of time frequency standard research, as it can immensely improve the performance of the time frequency standard.[8]

The Ramsey spectrum plays a crucial role in the development of precise atomic spectroscopy, atomic clocks, quantum information processing[9–11] and research on optical clocks.[12,13] Compared with the Rabi spectrum, the Ramsey spectrum can reduce the linewidth by about half, with the same clock detection time, and is insensitive to inhomogeneous excitation. These advantages have resulted in it being widely applied to not only atomic frequency standards to improve stability,[14–16] but Bose–Einstein condensates,[17] quantum computing,[18] information processing[11] and research on the laws of quantum mechanics.[19,20] Recently, numerous theoretical and experimental studies of optical Ramsey spectrum have shown that the modified Ramsey spectrum can also improve the accuracy of optical clocks by sharply reducing the probe Stark shift by hyper-Ramsey spectrum or autobalanced Ramsey spectroscopy.[21–28] Surprisingly, there are few reports about the optical Ramsey spectrum in optical lattice clocks and few papers on detailed study of the stability in optical lattice clocks based on the Rabi or Ramsey spectra, although the optical Ramsey spectrum has been successfully applied in optical lattice clocks.[16]

In this paper, we experimentally demonstrate the optical Ramsey spectrum in an ^{87}Sr optical lattice clock using a two $\pi/2$-pulse excitation scheme. The coherence time and dephasing time between the clock laser and the lattice-trapped atoms are measured based on the optical Ramsey and Rabi spectra, respectively. Furthermore, we theoretically and experimentally compare the stability between Ramsey and Rabi detection with the same clock duty cycle (the ratio of clock detection time to clock cycle T_c).

2. Experimental setup

After ^{87}Sr atoms are cooled to about 4 μK by two-stage laser cooling,[29] about 2.5×10^4 atoms are trapped in a horizontal 1D lattice, which is formed by overlapping the linearly polarized incident and its retroreflector beams at the center of the cold atomic gas. To reduce the frequency noise and drift, the 813 nm lattice laser is stabilized to an ultra-low expansion (ULE) cavity by Pound–Drever–Hall (PDH) technique, as shown in Fig. 1. Then, the lattice-trapped atoms are optically pumped into the $|^1S_0, m_F = +9/2\rangle$ stretched state by employing the circularly polarized 689 nm laser and about 1.2×10^4 atoms remain in the lattice after this process.

The clock transition of $5s^2\ ^1S_0 \rightarrow 5s5p\ ^3P_0$ is interrogated by the linearly polarized clock laser at 698 nm, which is PDH stabilized to a 10 cm ULE cavity with a finesse of 400000.[30] The frequency and power of the clock laser are controlled

†Corresponding author. E-mail: changhong@ntsc.ac.cn
© 2022 Chinese Physical Society and IOP Publishing Ltd

by changing the frequency of the input radio-frequency signal and the diffraction efficiency of an acousto-optic modulator (AOM), respectively. The Rabi and Ramsey sequences are shaped by an AOM driven at a frequency of 190 MHz by an arbitrary function generator that enables fast and precise control of the intensity, frequency and phase of the clock laser. During the clock transition, along the direction of gravity, a bias magnetic field with a magnitude of 400 mG is applied to spilt the adjacent Zeeman sub-levels by about 47 Hz to resolve the ten Zeeman sub-levels.[31] This bias magnetic field also defines the quantization axis along the gravity direction and the polarization of the clock laser and lattice laser is parallel to the gravity direction to excite the π-transition.

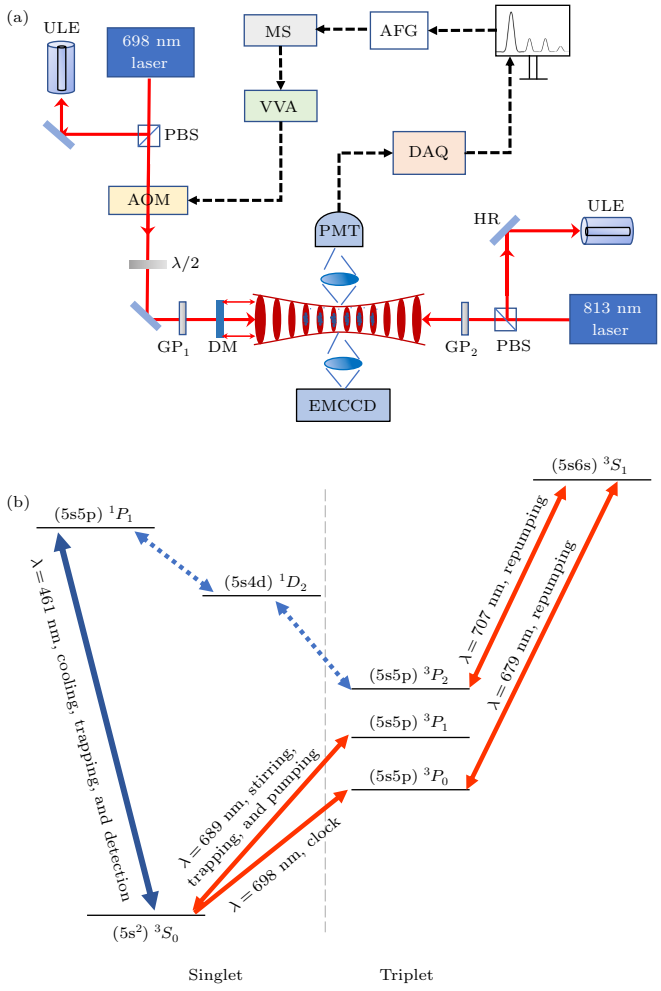


Fig. 1. Schematics of the experimental setup and energy levels. (a) Experimental setup of the lattice and the clock transition interrogation. AOM: acousto-optic modulator, AFG: arbitrary function generator, DAQ: data acquisition, MS: microwave switch, VVA: voltage variable attenuator, PMT: photomultiplier, HR: high reflector, GP_{1-2}: Glan–Taylor polarizers, PBS: polarizing beam splitters, DM: dichroic mirror, $\lambda/2$: half-wave plate, EMCCD: electron multiplying charge-coupled device. (b) Energy-levels schematic of an ^{87}Sr atom.

3. Results and discussion

3.1. Interrogation of the Ramsey spectrum

The interrogation scheme of the optical Ramsey spectrum with double $\pi/2$-pulses is shown in Fig. 2(a). The first $\pi/2$-pulse creates a coherent state between the ground and excited states. Then, the clock laser is turned off and atoms go through a free evolution period T, where the total wave function evolves with the atomic eigen energy and thus, a phase shift caused by the frequency difference between the clock transition and the clock laser accumulates.[9] The second $\pi/2$-pulse transfers the accumulated phase to the population difference between the $^1S_0$ and $^3P_0$ states, which allows effective measurement of the phase difference by detecting the excitation fraction. As there is no difference between the clock laser and the clock transition, the detected excitation fraction is at maximum. The optical Ramsey spectrum is obtained by scanning the clock laser frequency around the exact resonance and detecting the corresponding excitation fraction.

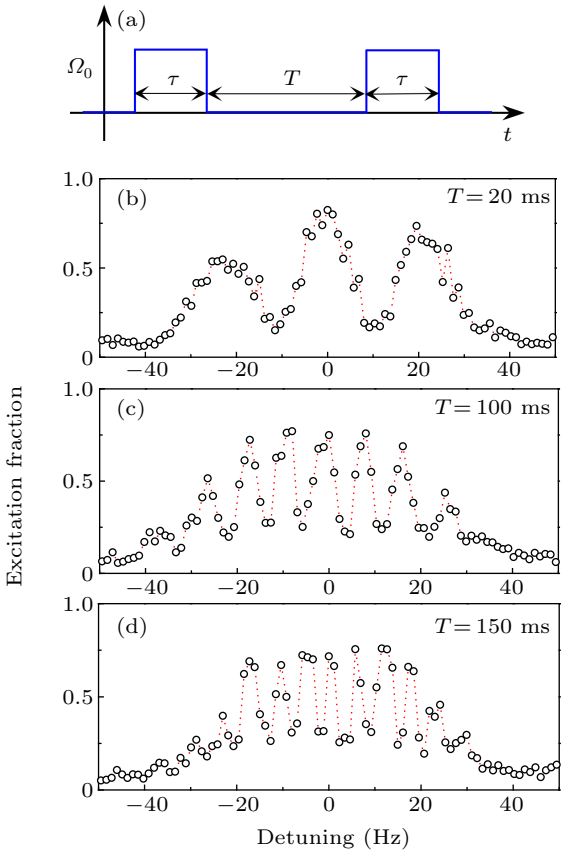


Fig. 2. Experimental interrogation of the optical Ramsey spectrum. (a) Detection sequence of the optical Ramsey spectrum. (b)–(d) Optical Ramsey spectra at free evolution periods of 20 ms, 100 ms, and 150 ms, respectively.

Figures 2(b)–2(d) experimentally interrogate the optical Ramsey spectrum, where the duration of the $\pi/2$-pulses is $\tau =$ 25 ms and the free evolution period T is 20 ms, 100 ms, and 150 ms, respectively. With the increase in T, more Ramsey interference fringes are observed, and the difference between the maximum and minimum excitation fraction around the center of the Ramsey spectrum reduces. In terms of long free evolution period T (when it exceeds 100 ms), the central Ramsey fringes are approximately sinusoidal. However, if the free evolution period is too long, the clock laser noise makes the interference fringes blurry, as shown in Fig. 2(d). With the optical

Ramsey spectrum, the Fourier-transform-limited full width at half maximum (FWHM) is $\Delta\nu_{\mathrm{Ramsey}} \approx 1/(2(\tau+T))$, which is about half of the Rabi spectrum of $\Delta\nu_{\mathrm{Rabi}} \approx 0.7987/T_{\mathrm{Ra}}$ as the Rabi detection time T_{Ra} is equal to the Ramsey detection time of $2\tau+T$.[32] By sinusoidally fitting the central Ramsey fringe, the FWHM of Figs. 2(b)–2(d) are 11.5(9) Hz, 4.5(6) Hz, and 2.9(6) Hz, respectively, agreeing with the corresponding Fourier-transform-limited linewidths of 11.1 Hz, 4 Hz, and 2.86 Hz, respectively.

3.2. Fringe contrast

The contrast $\mathbb{C}$ of Ramsey interference fringes can be defined as[33]

$$\mathbb{C} = P_{\max} - P_{\min}, \tag{1}$$

where $P_{\max}$ and $P_{\min}$ indicate the highest and lowest excitation around the central Ramsey fringes, respectively. Thus, the frequency sensitivity of the Ramsey spectrum to the clock laser noises is proportional to $\mathbb{C}$, indicating that higher stability is expected as the value of $\mathbb{C}$ is closer to 1.

As the number of interference fringes is below seven, $\mathbb{C}$ is obtained by only using maximum and minimum excitation of the central Ramsey fringe. When the free evolution period exceeds 100 ms, the fringes near the central Ramsey fringe will have a similar contrast, as shown in Figs. 2(c) and 2(d), and typically, the contrast is measured by the method shown in Fig. 3. Although the fringes of the Ramsey spectrum are blurry due to the noise of the clock laser, as the free evolution period is too long, contrast information can still be correctly extracted from the edges of the highest and lowest excitation fractions around the central interference fringes.

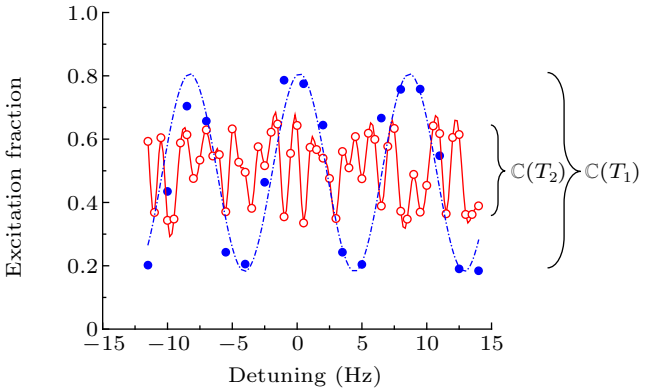


Fig. 3. Contrast measurement of the optical Ramsey spectrum. Circles are obtained with a free evolution period $T_1 = 120$ ms and the dotted line represents the sinusoidal fitting. Hollow circles are obtained with a free evolution period $T_2 = 600$ ms, and the red line indicates the direct connection of data as the clock laser noise washes out the sinusoidal nature of the fringes at such a long free evolution period (the sinusoidal fitting is unavailable in this case). Contrasts of $\mathbb{C}(T_1)$ and $\mathbb{C}(T_2)$ are extracted from the average floor and ceiling excitation fractions.

The contrast of the optical Ramsey spectrum is insensitive to the inhomogeneous excitation caused by thermal distribution of atoms in the lattice and the misalignment between the clock laser and lattice laser beams. However, atomic interaction, clock laser noises and inhomogeneous population between lattice sites can result in deterioration of the contrasts with the increase in T.[33] Figure 4(a) exhibits the Ramsey fringe contrast as a function of the free evolution period, where the $1/\mathrm{e}$ Gaussian decay time of contrasts indicates the coherence time of the atom–light interactions.[34] The coherence time represents the maximum time of coherent control of the clock transition, which gives the maximum accessible free evolution period of the clock transition interrogation. By fitting the experimental data of Fig. 4(a) with the Gaussian function, the coherence time is 340(23) ms.[34] Compared to the reported longest coherence time of 33(1) s, the coherence time in our system is mainly limited by the clock laser noise, atomic interaction and lattice light scattering.[34] At a Ramsey free evolution period that exceeds the coherence time, the Ramsey phase is randomized, which means that no useful phase information can be extracted from Ramsey detection, and thus, it is impossible to operate the clock.

In terms of Rabi detection, the maximum excitation also decreases with an increase in the clock laser duration, which is mainly caused by the inhomogeneous excitation. The $1/\mathrm{e}$ decay time of the amplitude of the Rabi oscillation is called dephasing time. However, the interrogation is also coherent, even though the Rabi detection time exceeds the dephasing time and the Rabi oscillation will revive as long enough detection time.[35] Figure 4(b) displays typical Rabi oscillation, where the low clock laser intensity is used to accurately obtain the dephasing time. By fitting the "SineDamp" function of $\exp\{-x/\omega_0\}\sin[\Omega(x-x_0)]$, dephasing time of 306 (11) ms is extracted, which is consistent with the result obtained from decaying contrast data of Ramsey detection within its 1σ uncertainty. Herein, x, Ω, ω_0, and x_0 represent the clock laser duration, Rabi frequency proportional to the square root of clock laser intensity, dephasing time and shifting offset.

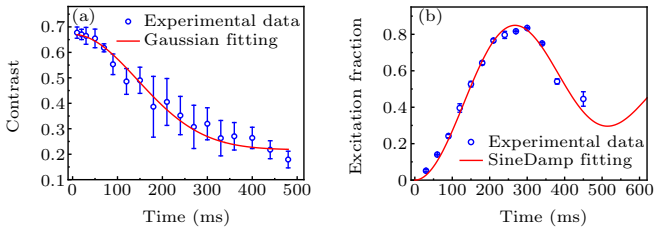


Fig. 4. Measurements of the coherence time and dephasing time. (a) Ramsey fringe contrast as a function of free evolution period. (b) Excitation fraction of Rabi spectrum as a function of interrogation time. Red solid line of (a) is obtained by the Gaussian function fitting and the red solid line of (b) is the fitting with the amplitude exponential-decaying sinusoidal function. Error bars indicate 1σ standard deviation of five measurements.

3.3. Measurement of stability

The clock stability is determined by the quantum projection noise (QPN) in single-ion optical clocks and the Dick noise in optical lattice clocks. The QPN limited stability can

be expressed by[30]

$$\sigma_{\mathrm{QPN}}(t) = \frac{\gamma}{2\sqrt{N}K_0 f_0}\sqrt{\frac{T_c}{t}}, \tag{2}$$

where γ is the linewidth; f is clock transition frequency; $K = |\mathrm{d}P_e/d\delta|\gamma$ is the maximum frequency sensitivity, where δ is the detuning of the clock laser frequency from the resonance, P_e indicates the excitation fraction at the detuning of δ, and for Rabi spectrum, $\mathbb{C}$ equals the maximum excitation fraction; $N \approx 1.2 \times 10^4$ is the number of atoms; $T_c = 950$ ms is the clock detection cycle and t is the averaging time.

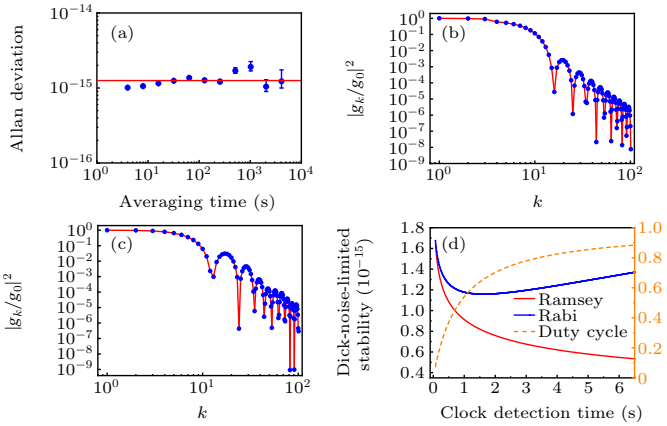


Fig. 5. Frequency flicker noise floor of the clock laser and calculation of the normalized Fourier coefficients. (a) Allan deviation of the clock laser frequency corrections after reducing the linear frequency drift. Red solid line is the linear fitting with a fixed slope of zero, which shows that the frequency flicker noise floor of the clock laser is 1.29×10^{-15}. (b) Squared magnitude of the normalized Fourier coefficients for Rabi detection with clock laser pulse duration of 100 ms and $T_c = 950$ ms. (c) Squared magnitude of the normalized Fourier coefficients for Ramsey detection with $T = 50$ ms, $\tau = 25$ ms, and $T_c = 950$ ms. (d) Calculation of Dick-noise-limited stability for Rabi and Ramsey interrogation. During calculation, dead time for both detection methods stays constant (0.85 s). Stability of Ramsey detection is more than 1.25 times the Rabi detection as the clock detection time is more than 0.85 s (corresponding to a clock duty cycle of 0.5).

According to Eq. (2), with the same clock detection time of 100 ms, γ is 8 Hz for Rabi spectrum and 6.6 Hz for Ramsey spectrum ($T = 50$ ms and $\tau = 25$ ms). The QPN limited stability is 7.7×10^{-17}@1 s and 5.7×10^{-17}@1 s for Rabi and Ramsey detection, respectively, indicating that the expected clock stability of Ramsey detection will be superior to that of Rabi detection. However, the Dick noise, originating from the down-converted high-frequency noise of the clock laser due to the periodic interrogation, usually dominates the stability of optical lattice clocks.[36] Using the flicker noise floor of the clock laser to approximate and infer the one-sided power spectral density of the clock laser, the Dick-noise-limited stability can be written as[36]

$$\sigma^2_{\mathrm{Dick}}(t) = \frac{\sigma^2_{\mathrm{clock}}}{2\ln 2}\frac{T_c}{t}\sum_{k=1}^{\infty}\frac{1}{k}\left|\frac{g_k}{g_0}\right|^2, \tag{3}$$

where σ_{clock} is the frequency flicker noise floor of the clock laser and given by analyzing the frequency correction signals (removing the linear frequency drift), as shown in Fig. 5(a) (the measured flicker noise floor is 1.29×10^{-15}); g_k is the Fourier coefficients of the frequency-sensitive function.[36] Figures 5(b) and 5(c) demonstrate the squared magnitude of the normalized Fourier coefficients of Rabi and Ramsey detection, respectively. Thus, the Dick-noise-limited stabilities of Rabi and Ramsey detection are 1.59×10^{-15} and 1.53×10^{-15}, respectively, indicating that the influence of the QPN is negligible. Figure 5(d) demonstrates the Dick-noise-limited stability of Rabi and Ramsey detection as a function of clock detection time and indicates that with increasing the clock detection time, the stability of Ramsey detection will be obviously better than Rabi detection.

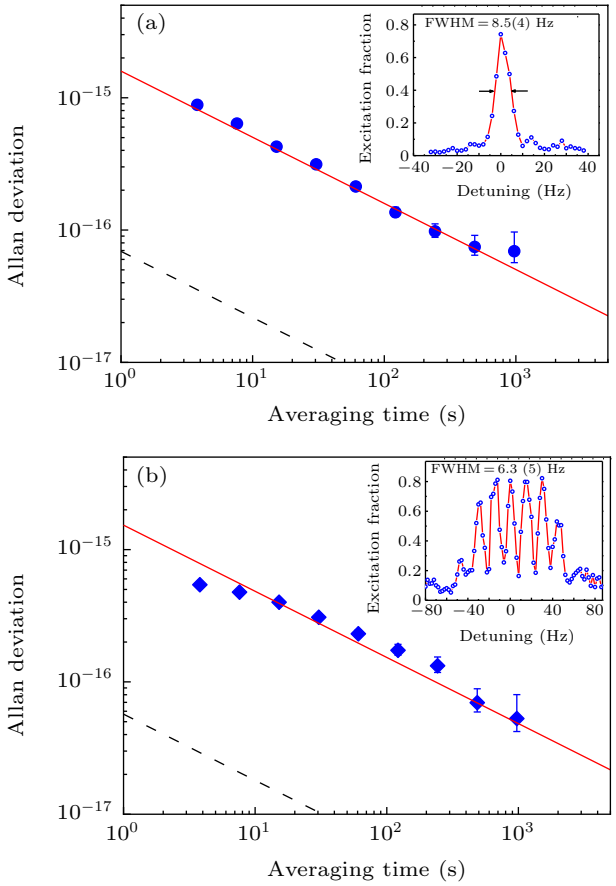


Fig. 6. Measurements of single clock stability using the interleaved stabilization method. (a) Stability using the 8.5 Hz Rabi spectrum. Inset shows the Rabi spectrum with a clock laser pulse duration of 100 ms. (b) Stability using the 6.3 Hz Ramsey spectrum. Inset demonstrates the Ramsey spectrum with T =50 ms and τ =25 ms. In both (a) and (b), the clock detection cycle is 950 ms ($T_c = 950$ ms). Red solid and black dashed lines represent the calculated Dick-limited stability and QPN-limited stability, respectively.

Under the same parameters, with the previous calculations, the stability of the ^{87}Sr optical lattice clock is experimentally measured by Rabi detection and Ramsey detection, respectively. Here, the stability of a single clock is inferred from the single-peak interleaved self-comparison stability by dividing it by a factor of 2.[37–39] The measured stability is 1.71×10^{-15}@1 s for Rabi detection and 1.62×10^{-15}@1 s for Ramsey detection. The experimentally measured stability

is slightly lower than the corresponding calculations of Dick-noise-limited stability, which may be caused by the clock not always being able to probe the atomic resonance line at a half-width point where the frequency sensitivity is at maximum. Thus, only the theoretical calculation is considered.

4. Conclusion and perspectives

In summary, based on the ^{87}Sr optical lattice clock, the optical Ramsey is realized, and the corresponding linewidths agree well with theoretical expectation. The coherence time of 340(23) ms is extracted from the $1/e$ Gaussian decay of the Ramsey contrast, and is consistent with the dephasing time of 306(11) ms obtained by fitting the damping Rabi oscillation. With the same clock duty cycle, the stability of our clock is experimentally measured, and the results agree with the corresponding theoretical calculations of Dick-noise-limited stability. The clock stability will not be obviously improved by using the narrower Ramsey spectrum, until the clock duty cycle is near or beyond 0.5, or the Dick effect is made lower than the QPN by reducing the clock laser noise,[38] using the zero-dead-time clock technique[13] or the quantum non-demolition measurement.[12] It is worth mentioning that Ramsey detection is quite sensitive to phase variation between the clock laser and the atoms, indicating that precise control of the clock laser phase is critical, otherwise, unexpected systematic shift may occur and deteriorate the clock accuracy.

Acknowledgments

Project supported by the National Natural Science Foundation of China (Grant No. 61775220), the Key Research Project of Frontier Science of the Chinese Academy of Sciences (Grant No. QYZDB-SSW-JSC004), and the Strategic Priority Research Program of the Chinese Academy of Sciences (Grant No. XDB21030100).

References

[1] Wineland D J 2013 *Ann. Phys.* **525** 739
[2] Haroche S 2013 *Rev. Mod. Phys.* **85** 1083
[3] Dow J M, Neilan R E and Rizos C 2009 *J Geod* **83** 689
[4] Derevianko A and Pospelov M 2014 *Nat. Phys.* **10** 933
[5] Mehlstäubler T E, Grosche G, Lisdat Chr, Schmidt P O and Denker H 2018 *Rep. Prog.* **81** 064401
[6] Lisdat C, Grosche G, Quintin N, *et al.* 2016 *Nat. Commun.* **7** 12443
[7] Targat R Le, Lorini L, Coq Y Le, *et al.* 2013 *Nat. Commun.* **4** 2109
[8] Milner W R, Robinson J M, Kennedy C J, *et al.* 2019 *Phys. Rev. Lett.* **123** 173201
[9] Ramsey and Norman F 1950 *Phys. Rev.* **78** 695
[10] Liu L, Lü D S, Chen W B, *et al.* 2018 *Nat. Commun.* **9** 2760
[11] Schindler P, Nigg D, Monz T, Barreiro J T, Martinez E, Wang S X, Quint S, Brandl M F, Nebendahl V, Roos C F, Chwalla M, Hennrich M and Blatt R 2013 *New J. Phys.* **15** 123012
[12] Bowden W, Vianello A, Hill I R, Schioppo M and Hobson R 2020 *Phys. Rev. X* **10** 041052
[13] Schioppo M, Brown R C, McGrew W F, Hinkley N, Fasano R J, Beloy K, Yoon T H, Milani G, Nicolodi D, J. Sherman A, Phillips N B, Oates C W and Ludlow A D 2016 *Nat. Photon.* **11** 48
[14] Heavner T P, Donley E A, Levi F, Costanzo G, Parker T E, Shirley J H, Ashby N, Barlow St and Jefferts S R 2014 *Metrologia* **51** 174
[15] Wang Q, Wei R and Wang Y Z 2018 *Acta Phys. Sin.* **67** 163202 (in Chinese)
[16] Takamoto M, Ushijima I, Ohmae N, Yahagi T, Kokado K, Shinkai H and Katori H 2020 *Nat. Photon.* **14** 411
[17] Donley E A, Claussen N R, Thompson S T and Wieman C E 2002 *Nature* **417** 529
[18] Lim J, Lee H G, Lee S, Park C Y and Ahn J 2014 *Sci. Rep.* **4** 5867
[19] Gleyzes S, Kuhr S, Guerlin C, Bernu J, Deléglise S, Hoff U B, Brune M, Raimond J M and Haroche S 2007 *Nature* **446** 297
[20] Safronova M S, Budker D, DeMille D, Jackson K D F, Derevianko A, and Clark C W 2018 *Rev. Mod. Phys.* **90** 025008
[21] Yudin V, Taichenachev A V, Oates C W, Barber Z W, Lemke N D, Ludlow A D, Sterr U, Lisdat C and Riehle F 2010 *Phys. Rev. A* **82** 11804
[22] Shuker M, Pollock J W, Boudot R, Yudin V I, Taichenachev A V, Kitching J and Donley E A 2019 *Appl. Phys. Lett.* **114** 141106
[23] Yudin V I, Basalaev M Yu and Taichnachev A V 2017 *J. Phys. Conf. Ser.* **793** 012034
[24] Shuker M, Pollock J W, Kitching J, Donley E A, Yudin V I, Boudot R and Taichenachev A V 2019 *Joint Conference of the IEEE International Frequency Control Symposium an European Frequency and Time Forum*, April 14–18, 2019, Orlando, United States, p. 978
[25] Huntemann N, Lipphardt B, Okhapkin M, Tamm C, Peik E, Taichenachev A V and Yudin V I 2012 *Phys. Rev. Lett.* **109** 213002
[26] Shuker M, Pollock J W, Boudot R, Yudin V I, Taichenachev A V, Kitching J and Donley E A 2019 *Phys. Rev. Lett.* **122** 113601
[27] Sanner C, Huntemann N, Lange R, Tamm C and Peik E 2018 *Phys. Rev. Lett.* **120** 053602
[28] Yudin V, Taichenachev A, Basalaev M Y, Zanon-Willette T, Pollock J W, Shuker M, Donley E A and Kitching J 2017 *Phys. Rev. Appl.* **9** 054034
[29] Wang Y B, Yin M J, Ren J, Xu Q F, Lu B Q, Han J X, Guo Y and Chang H 2018 *Chin. Phys. B* **27** 023701
[30] Lu X T, Zhou C H, Li T, Wang Y B and Chang H 2021 *Appl. Phys. Lett.* **117** 231101
[31] Boyd M M, Zelevinsky T, Ludlow A D, Blatt S, Zanon-Willette T, Foreman S M and Jun Y 2011 *Phys. Rev. A* **76** 022510
[32] Marmet L and Madej A A 2000 *Can. J. Phys* **78** 495
[33] Martin M J 2013 *Quantum Metrology and Many-Body Physics: Pushing the Frontier of the Optical Lattice Clock* (Ph.D. Dissertation) (Colorado: University of Colorado) p. 206
[34] Aaron W Y, William J E, William R M, Dhruv K, Matthew A N, Eric O, Nathan S, Jun Y and Adam M K 2020 *Nature* **588** 408
[35] Ludlow A D 2008 *The Strontium Optical Lattice Clock: Optical Spectroscopy with Sub-Hertz Accuracy* (Ph.D. Dissertation) (Colorado: University of Colorado) p. 195
[36] Dick G J 1987 *Proceedings of the 19th Annual Precise Time and Time Interval Meeting*, December 1–3, 1987, Los Angeles, USA, p. 133
[37] Nicholson T L, Martin M J, Williams J R, Bloom B J, Bishof M, Swallows M D, Campbell S L, Ye J 2012 *Phys. Rev. Lett.* **109** 230801
[38] Lin Y G, Wang Q, Li Y, Meng F, Lin B K, Zang E J, Sun Z, Fang F, Li T C and Fang Z J 2015 *Chin. Phys. Lett.* **32** 090601
[39] Liu Hu, Zhang X, Jiang K L, Wang J Q, Zhu Q, Xiong Z X, He L X and Lyu B L 2017 *Chin. Phys. Lett.* **34** 020601